Electronic Supplementary Material (ESI) for ChemComm.

This journal is © The Royal Society of Chemistry 2024

Supporting Information

Sensitive subcellular scale and real-time detection of hydrogen peroxide by W-doped Pt microelectrode

Shaohui Lei [a], Zhuo Zou [a], Kangling Tian [a], Yan Zheng [a], Mei Ding [a], Guangxuan Hu [a], Hong Bin Yang [a], Chunxian Guo [a], Changming Li [a] *, Fang Xin Hu [a] *

[a] *School of Materials Science and Engineering, Suzhou University of Science and Technology, Suzhou 215009, China*

*Correspondence author: ecmli@mail.usts.edu.cn (CM Li), hufx278@usts.edu.cn (FX Hu)

1. Experimental Details

1.1 Materials and reagents

Graphene oxide (GO) was purchased from Xianfeng Nano Company, sodium chloride (NaCl) and chloroplatinate hexahydrate ($H_2PtCl_6 \cdot 6H_2O$) were purchased from Aladdin reagent network, ethylene glycol ($(CH_2OH)_2$) was purchased from Aladdin reagent network, and tungsten (W) powder was purchased from Hunan Outai Rare Metals Co., LTD.

Phorbol 12-myristate 13-acetate (PMA) was purchased from the Aladdin Reagent, The Catalase (CAT from bovine liver) was purchased from the Sigma, Medium was obtained from Key GEN Bio TECH, RPMI-1640 medium, FBS Adamas life Fetal Bovine Serum, Trypsin-EDTA produced by Gibco (0.05%), PBS buffer solution (0.01 M, pH = 7.4) is from Qingdao Hi-tech Industrial Park Hope Bio-technology Co., Ltd., (Qingdao, China).

1.2 Instruments

Nano-electric probe (PE100 tip size 0.7 μm) produced by Jiangsu Rayme Biotechnology Co., Ltd. (Wuxi, China). Saturated calomel electrode (SCE, CHI 150) and platinum wire electrode (CHI 115) were purchased from CH Instruments Co., Ltd. (Shanghai, China). Subcellular level detection is conducted with a Live-time Single Cell Multi-Mode Analyzer (RMA-MO1) produced by Jiangsu Rayme Biotechnology Co., Ltd., (Wuxi, China).

1.3 Cell culture

HeLa cells are purchased from Procell Life Co., Ltd. (Wuhan, China). The culture medium of HeLa cells was prepared from DMEM and 10% fetal cattle and 1% double antibody, and the cells were washed three times with sterile PBS. Trypsin was then added and the cells were digested for two minutes. The cells were then placed into a centrifuge at 1500 rmp and centrifuged for 5 min. The supernatant after centrifugation was reversed, 4 mL of culture was added, and cells were resuspended by blow. Finally, 1 mL of cell suspension was absorbed into the plate, and 4 mL of culture was added. Light shaking so that the cells were evenly distributed at the bottom of the plate. Put them into an incubator and incubated at 25 °C for 48 h.

1.4 Preparation of biosensor

Firstly, 10 mg of graphene (GO) was weighed and dispersed in 10 mL of deionized

water and ultrasound was performed for 1 h to form a stable GO colloidal system. Then 20 mL of $(CH_2OH)_2$ and 5 mg of metal precursor $H_2PtCl_6 \cdot 6H_2O$ were added, stirred at room temperature for 30 min, and finally stirred in an oil bath at 100 ℃ for 6 h. It is then separated by centrifuge, washed 5 times with deionized water, and dried in a vacuum drying oven for 12 h. Pt-GO material can be obtained. The heat treatment products were washed with deionized water, NaCl was removed, and freeze-dried to obtain graphene-supported metal platinum material (Pt-GO). Using the same method, 20 wt% W powder of 5 mg $H_2PtCl_6 \cdot 6H_2O$, i.e. 1 mg, was mixed with 20 mL $(CH_2OH)_2$ and GO colloidal system to finally obtain W-doped graphene-supported metallic platinum material (Pt-W-GO). Metal W powder with mass fraction of H_2O_2 6.8 wt% was weighed and reacted with it for 3 min to obtain a colorless and transparent solution. Then, stir and heat in a closed container at 100 ℃ for 2 h to obtain yellow solution, and stir for 5 h to produce yellow precipitation. The solvent evaporates to produce dry powder. Finally, it is mixed with 20 mL $(CH_2OH)_2$ and 10 mL GO colloidal system to obtain W-GO material. The Pt-W-GO was prepared as a 2 mg mL^{-1} aqueous solution and sonicated for 20 mins. Three-electrode system is used with nano-electric probe with deposited Au on it as the working electrode, SCE (1 mol L^{-1} KCl) as the reference electrode, and the platinum wire electrode as the counter electrode. Potentiometric Stripping Analysis (PSA) method was applied to modify the nano-electric probe with Pt-W-GO material with a deposition potential as -1.2 V, for 1200 s, The PBS used for the experiment was 0.01 M.

1.5 In situ detection of H_2O_2 released by HeLa cells at subcellular level

Experiments were performed with a Live-time Single Cell Multi-Mode Analyzer, which contains an inverted microscope to found a single HeLa cell, and an electrochemical signal detection and processing system. The microelectrode tips were adjusted to different locations of cells including extracellular, cytoplasm and nucleus. 10 μL PMA, or mixture of PMA and CAT were applied as the stimulation drugs for HeLa cells.

2. Supplementary Figures and Tables

- **Figure S1.** A photo of the microelectrode.
- **Figure S2.** The SEM and EDS of the Pt-W-GO.

- **Figure S3.** The SEM and EDS of the Pt-GO.
- **Figure S4.** The SEM and EDS of the W-GO.
- **Figure S5.** SEM of unmodified microelectrode.
- **Figure S6.** XPS overall survey of Pt-W-GO.
- **Figure S7.** CV of the unmodified microelectrode after the addition of H_2O_2.
- **Figure S8.** The CV of the Pt-GO@ME after the addition of H_2O_2.
- **Figure S9.** The CV of the W-GO@ME after the addition of H_2O_2.
- **Figure S10.** CV of 7.06 mM H_2O_2 modified electrode with different materials.
- **Figure S11.** LSV curves of the microelectrode in response to H_2O_2 with Pt-GO@ME
- **Figure S12.** LSV curves of the microelectrode in response to H_2O_2 with W-GO@ME
- **Figure S13.** The EIS of the blank electrode and the Pt-W-GO@ME.
- **Figure S14.** I-t curves of different doping ratios of W after adding 10 uL 3% H_2O_2.
- **Figure S15.** Current values of the CV after adding 0 mM and 7.06 mM of H_2O_2 with Pt-W-GO@ME fabricated with different deposition voltages by PSA method.
- **Figure S16.** Applied potential optimization for Pt-W-GO@ME I-t response toward H_2O_2.
- **Figure S17.** Current change value of CV at different pH.
- **Figure S18.** The I-t curves of Pt-W-GO@ME for detection of H_2O_2.
- **Figure S19.** Response time of the Pt-W-GO@ME toward H_2O_2.
- **Figure S20.** Stability of Pt-W-GO@ME.
- **Table 1.** Comparison of the performance of the different materials and this work.
- **Video S1.** The process of microelectrode detection at cellular scale under microscope.

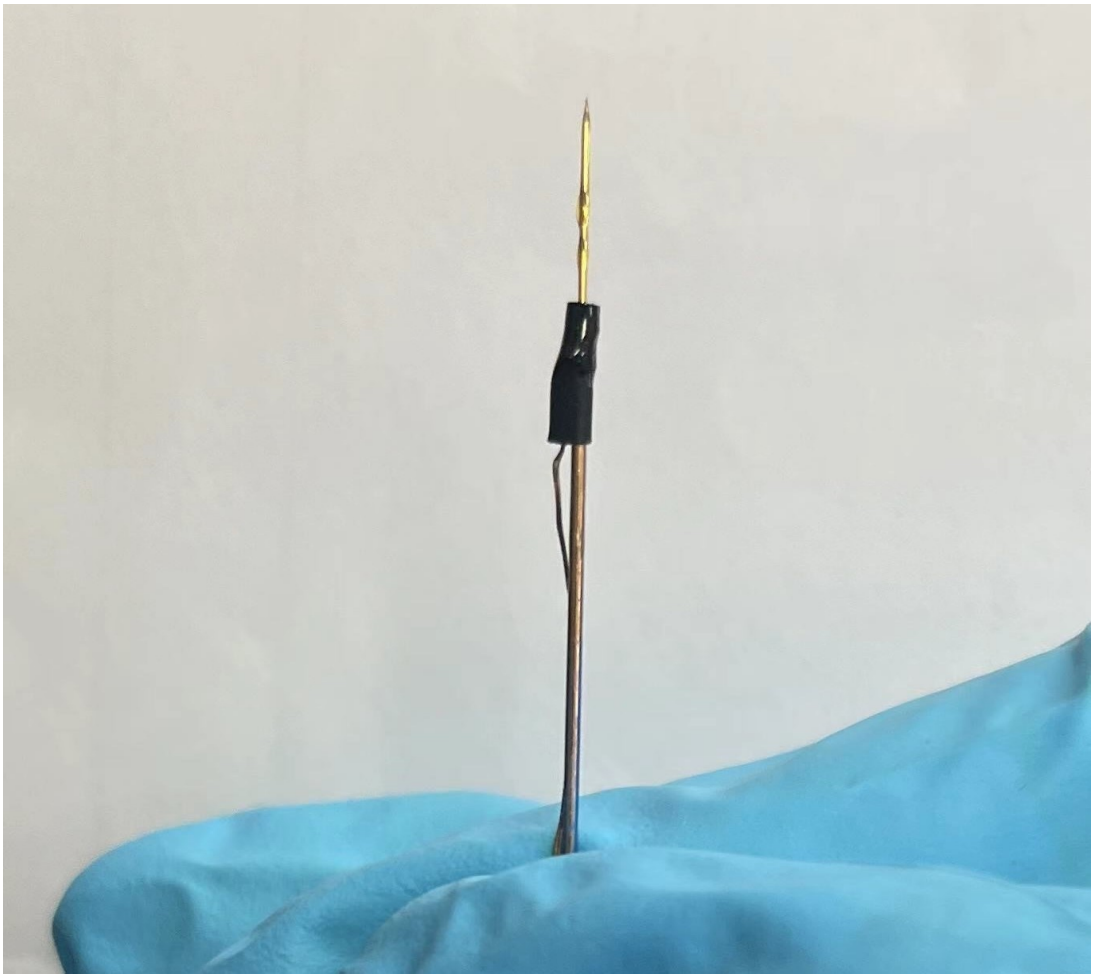

Fig. S1. A photo of the microelectrode.

The microelectrode used in this work is a nano-electric probe purchased from Jiangsu Rayme Biotechnology Co., LTD., with a diameter below 0.7 μm. The nanoelectric probe is a glass capillary tube with a gold-plated surface.

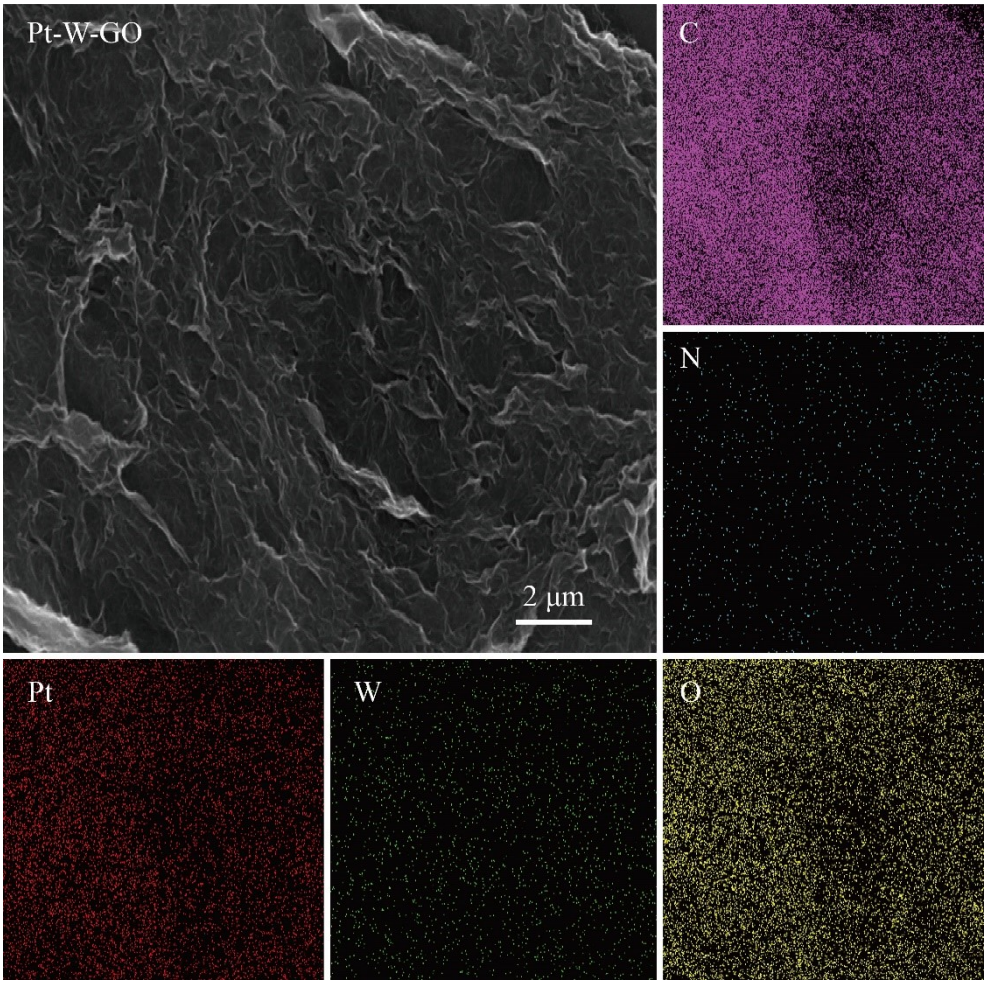

Fig. S2. The SEM and EDS of the Pt-W-GO.

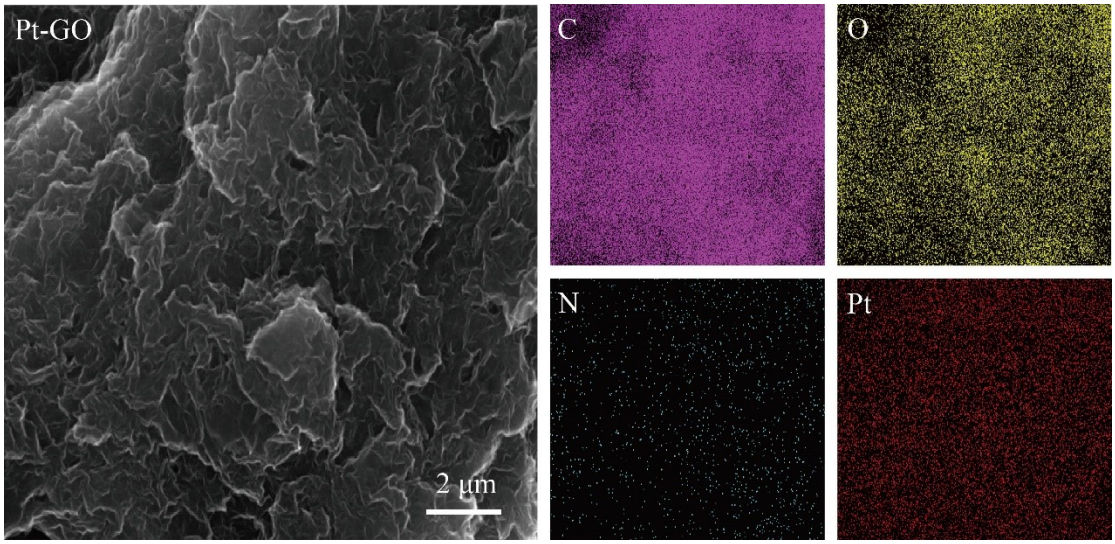

Fig. S3. The SEM and EDS of the Pt-GO.

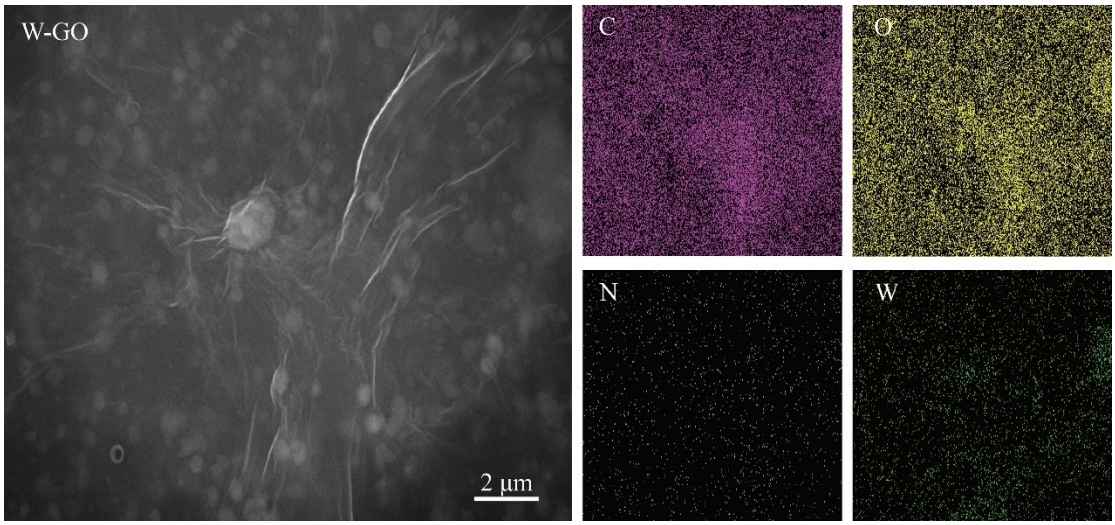

Fig. S4. The SEM and EDS of the W-GO.

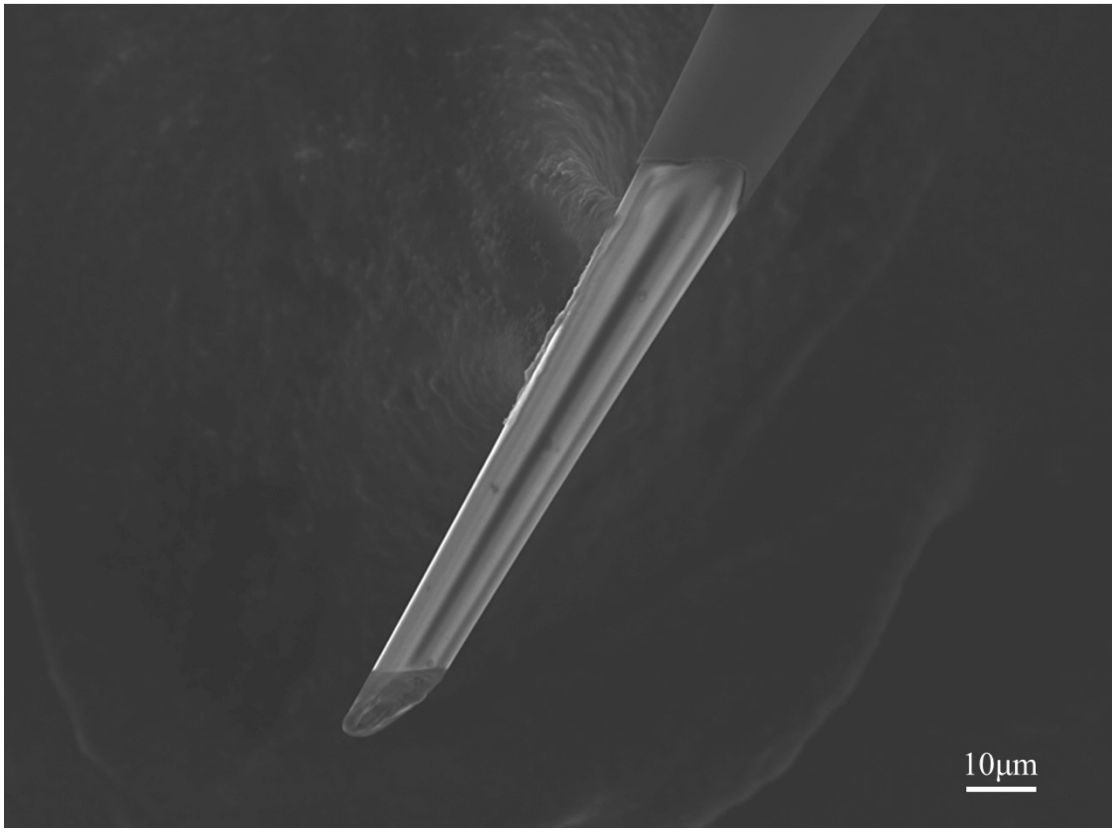

Fig. S5. SEM of unmodified microelectrode.

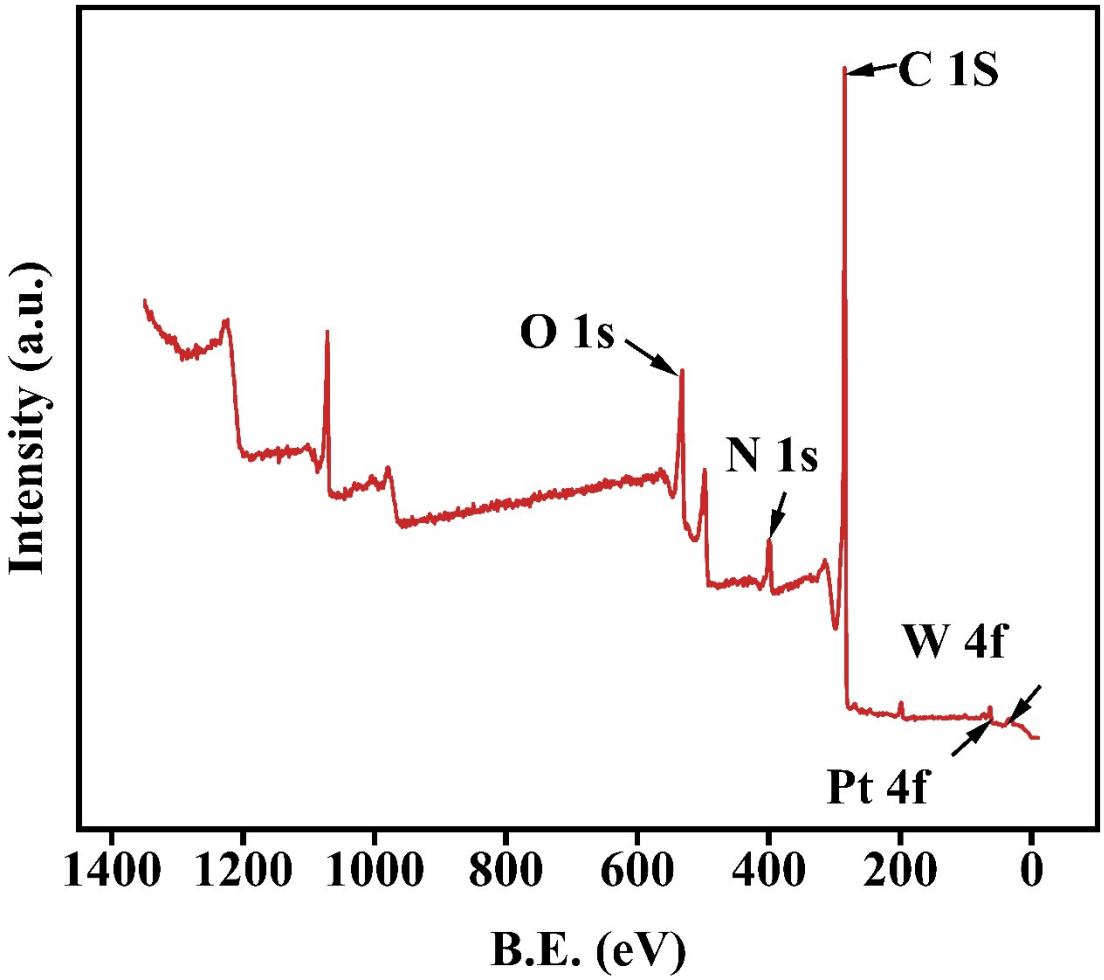

Fig. S6. XPS overall survey of Pt-W-GO.

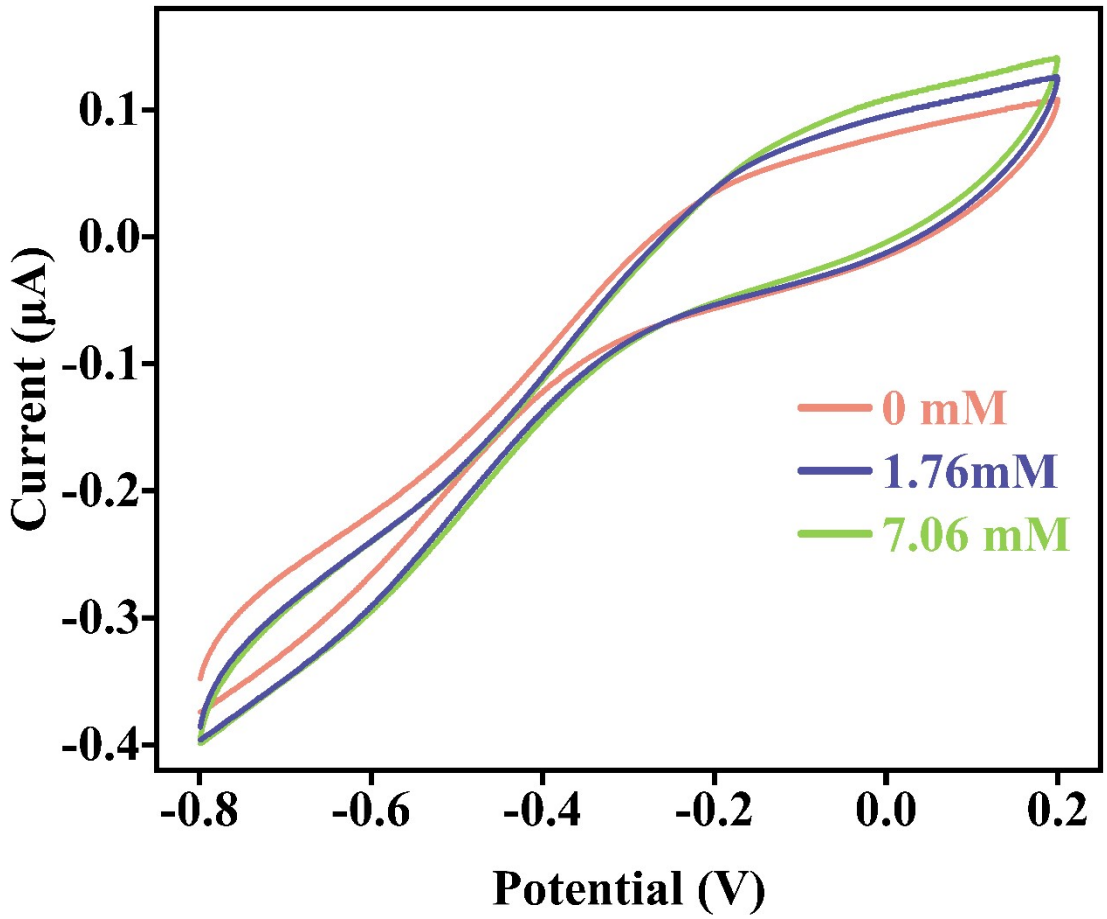

Fig. S7. The CV of the unmodified microelectrode after the addition of 3% H_2O_2.

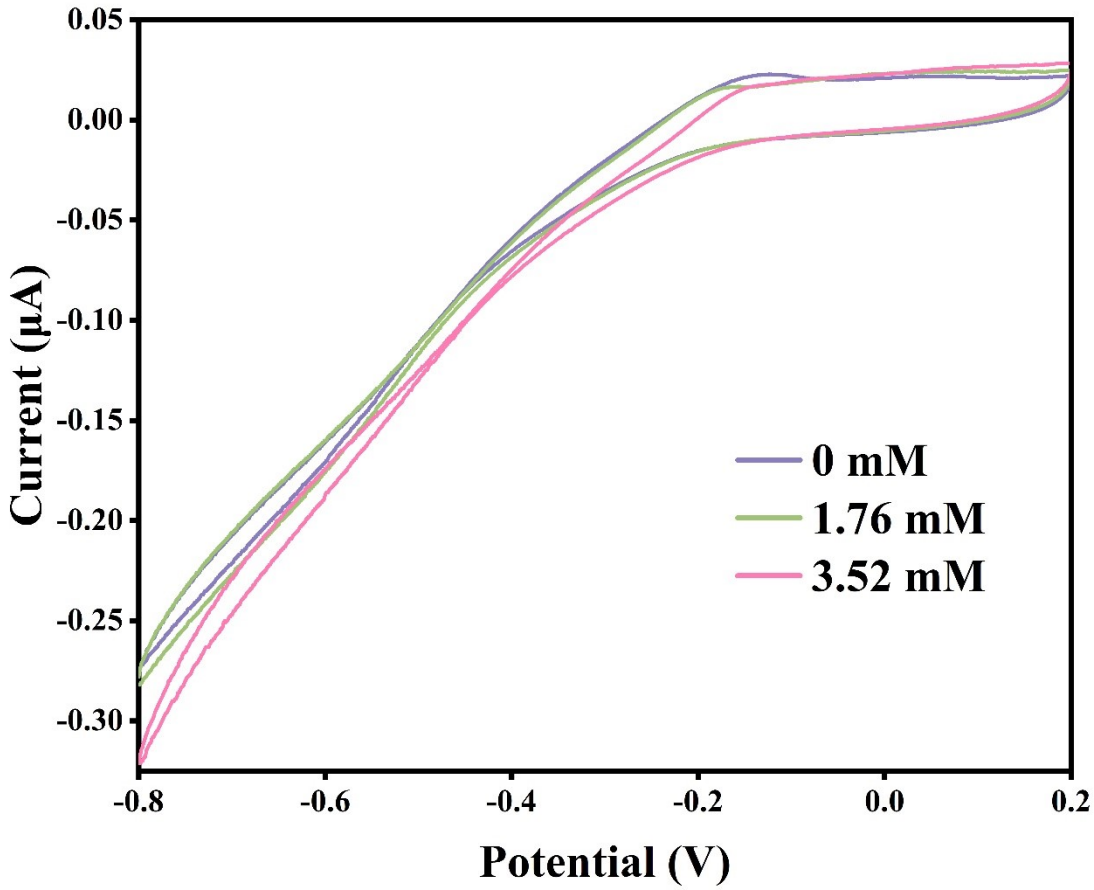

Fig. S8. The CV of the Pt-GO@ME after the addition of 3% H_2O_2.

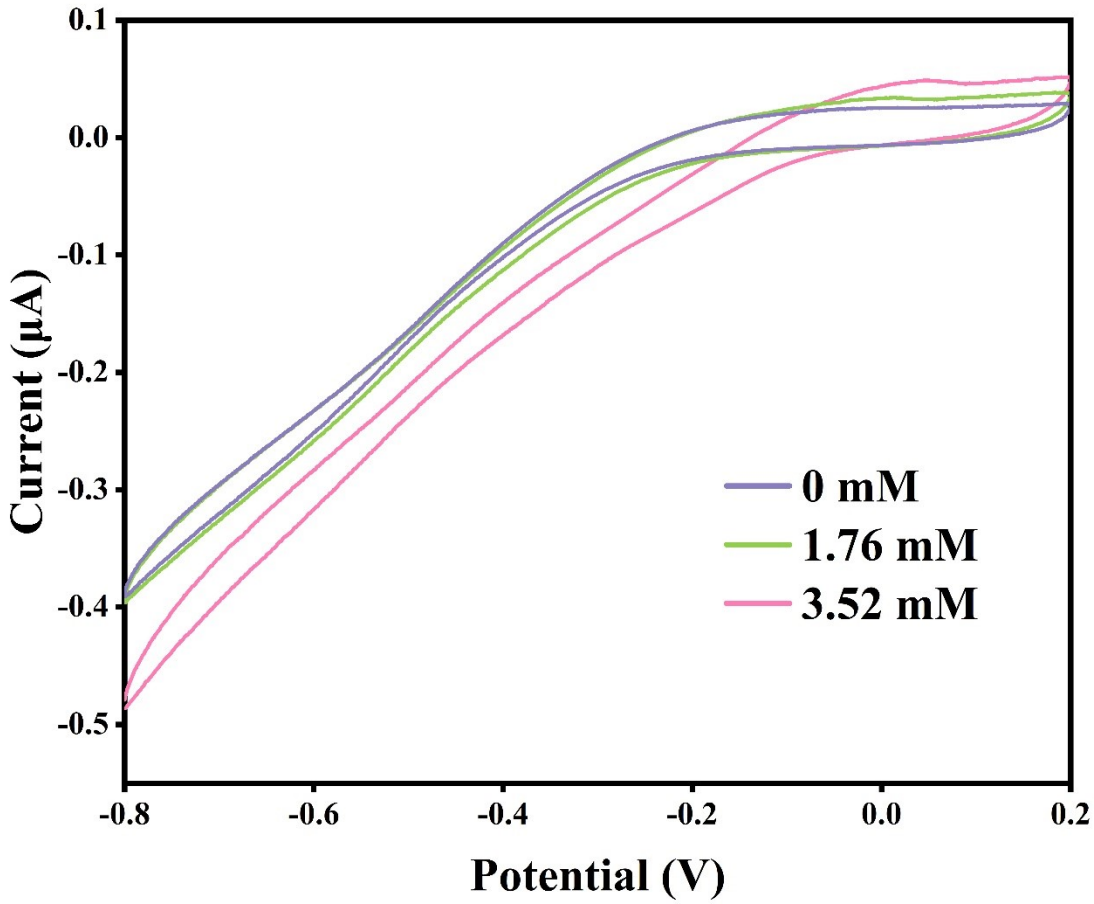

Fig. S9. The CV of the W-GO@ME after the addition of H_2O_2.

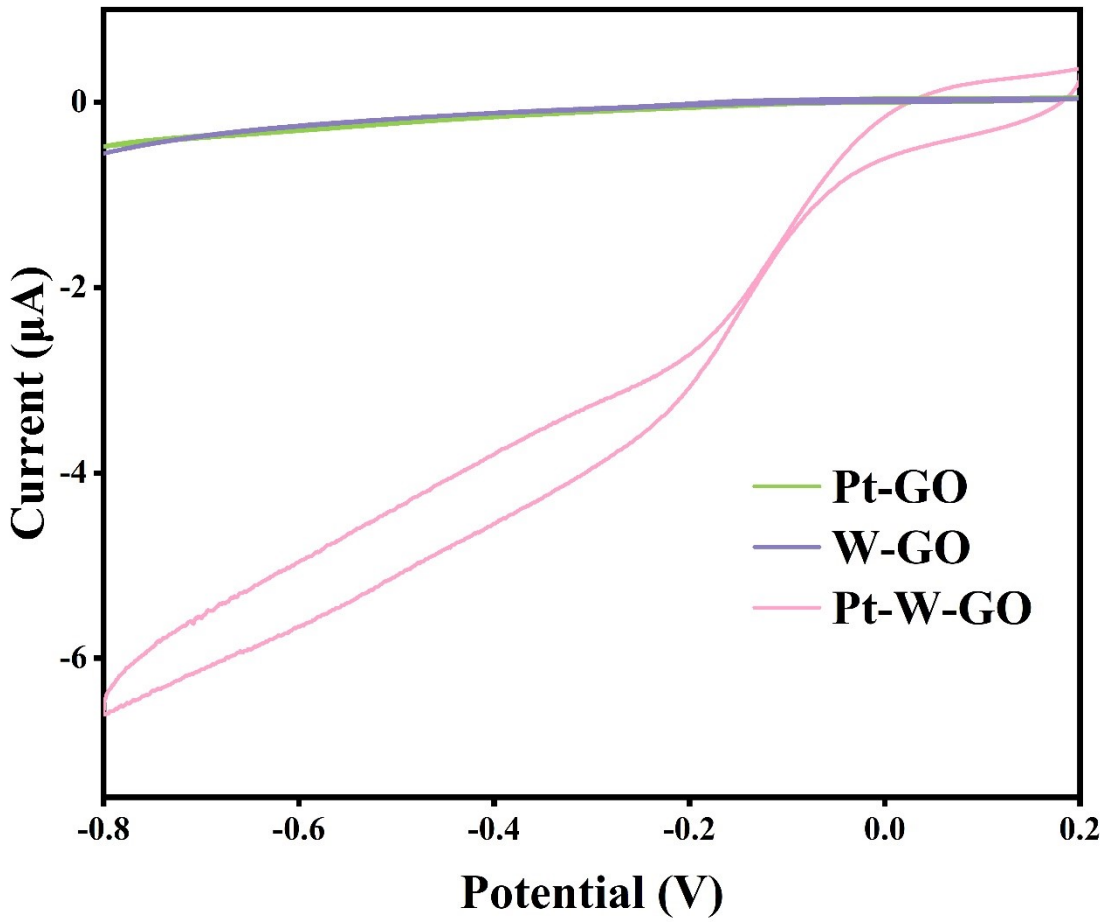

Fig. S10. CV of 7.06 mM H_2O_2 modified electrode with different materials.

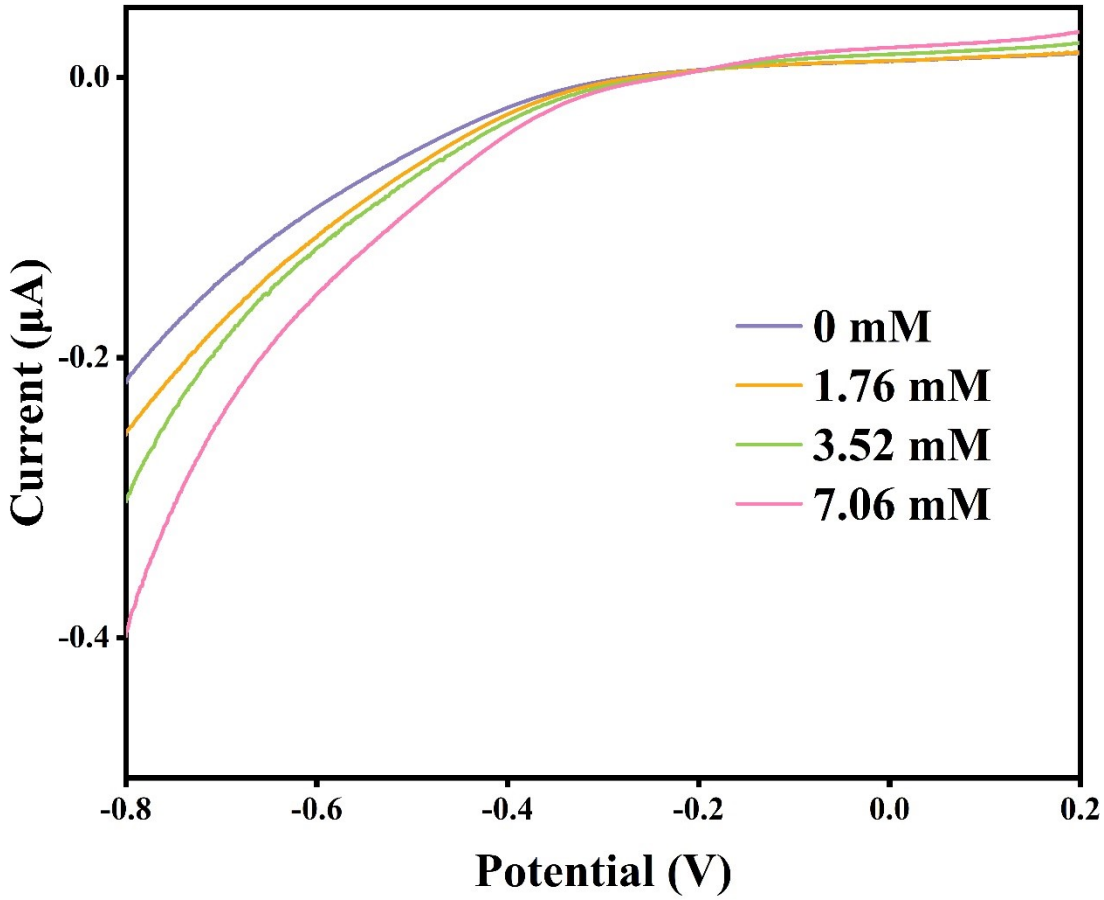

Fig. S11. LSV curves of the microelectrode in response to H_2O_2 with Pt-GO@ME.

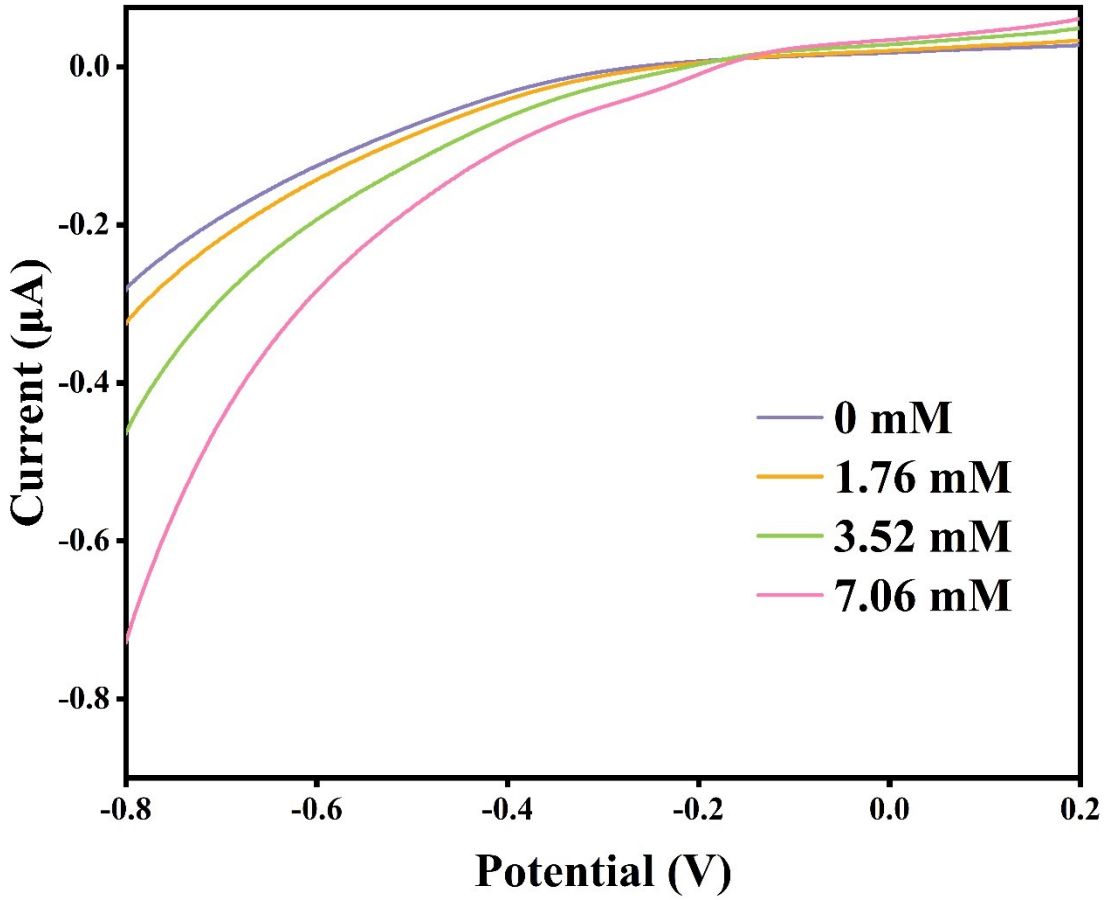

Fig. S12. LSV curves of the microelectrode in response to H_2O_2 with W-GO@ME.

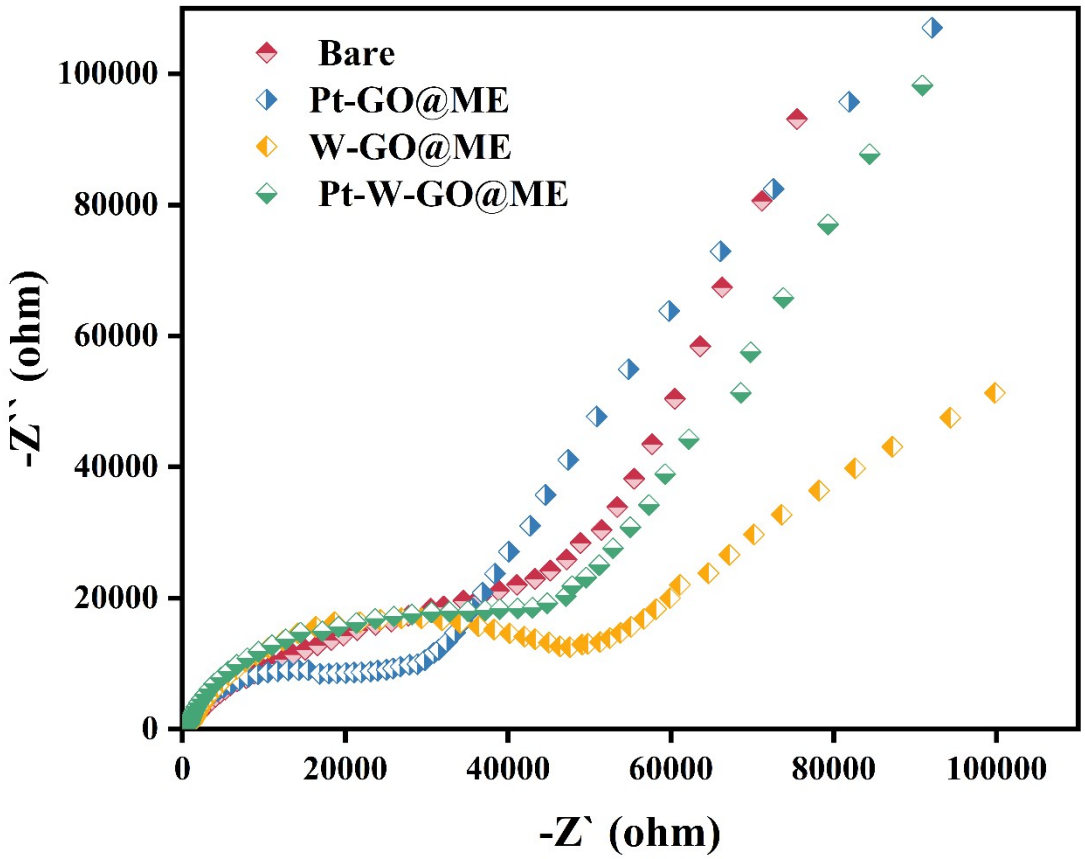

Fig. S13. The EIS of the blank electrode and the Pt-W-GO@ME.

The electrochemical impedance spectra of the modified and unmodified electrodes are shown in Fig. S13. The EIS spectrum is quasi-semicircular at high frequencies, in part due to the electron transfer limitation process. From left to right Pt-GO, Bare (unmodified electrode), Pt-W-GO and W-GO arc inflection point abscis are 31500, 41100, 44800 and 49800, indicating that the impedance increases with the radius of the arc. Due to the excellent conductivity of Pt, its impedance in the high frequency region is lower than that of Bare. Due to the fixation of Pt-W-GO on the surface of the microelectrode, the charge transfer resistance increases, making the impedance of Pt-W-GO@ME in the high frequency region higher than that of Bare. Finally, the conductivity of W is lower than that of Pt, so the impedance of W-GO@ME will be large.

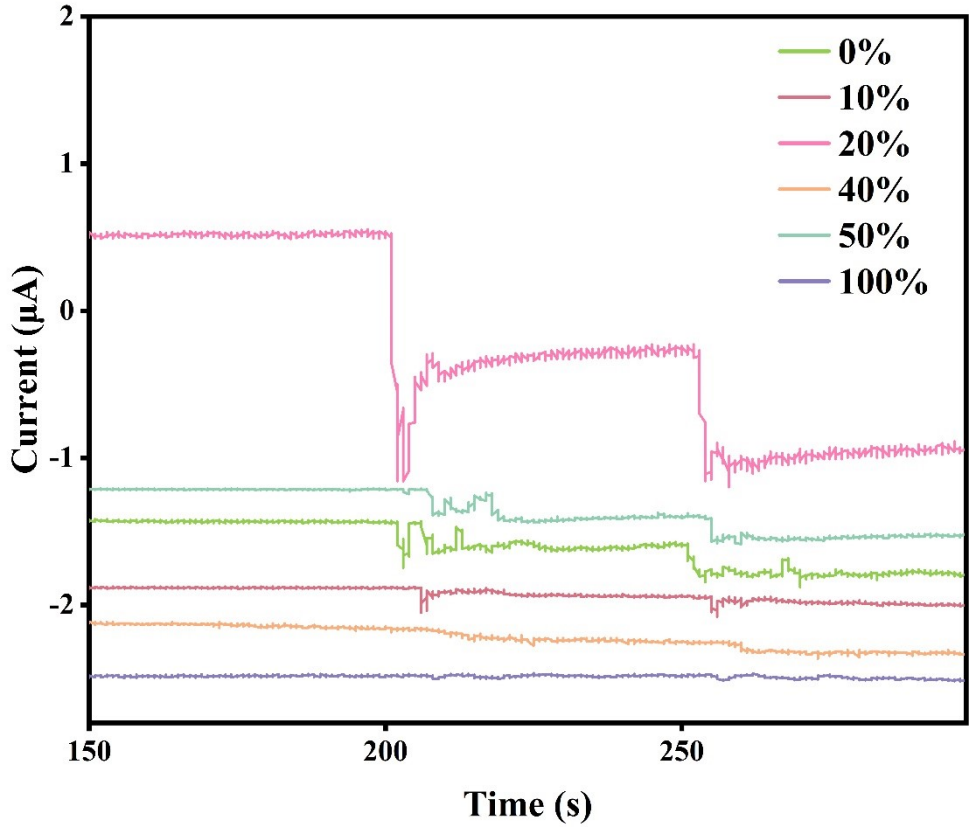

Fig. S14. I-t curves of different doping ratios of W after adding 0.882 M H_2O_2

As shown in Fig. S14, we adjust the doping proportion of W in Pt, where the percentage represents the mass proportion of W relative to Pt, and optimized the doping ratio of W, including 0 wt%, 10 wt%, 20 wt%, 50 wt% and 100 wt%, where percentage represents the mass ratio of W to Pt. Subsequently, the synthesized Pt-W-GO materials with different ratio of W was successfully deposited uniformly on microelectrodes using established methods. Then, I-t method was applied to investigate the response performance of modified microelectrodes toward 0.882 M H_2O_2. With the increase of W doping ratio from 0 % to 20 %, we observe that the I-t response first gradually increases, however, the current response decreases when the ratio further increases above 20 wt%. Results show that Pt-W-GO materials with W doping 20 wt% behaved the best performance.

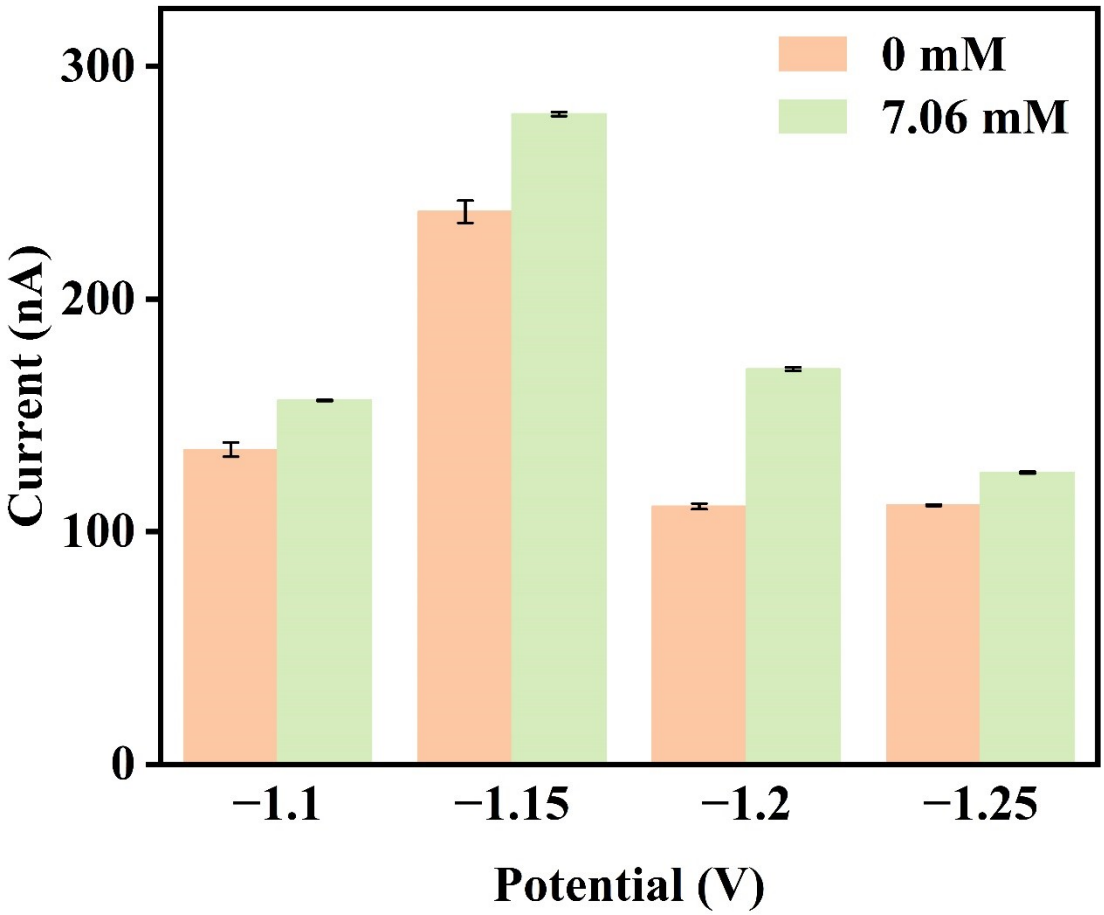

Fig. S15. Current values of the CV after adding 0 mM and 7.06 mM of H_2O_2 with Pt-W-GO@ME fabricated with different deposition voltages by PSA method.

In order to improve the catalytic performance of Pt-W-GO@ME toward H_2O_2, we optimized the deposition potential of PSA method. CV responses toward H_2O_2 of Pt-W-GO@ME fabricated with different deposition potentials were shown in Fig. S15, recording the changes in response to 7.06 mM H_2O_2. Results show that the current response reached the biggest when the potential was -1.2 V. So, -1.2 V was chosen as the deposition potential for further experiments.

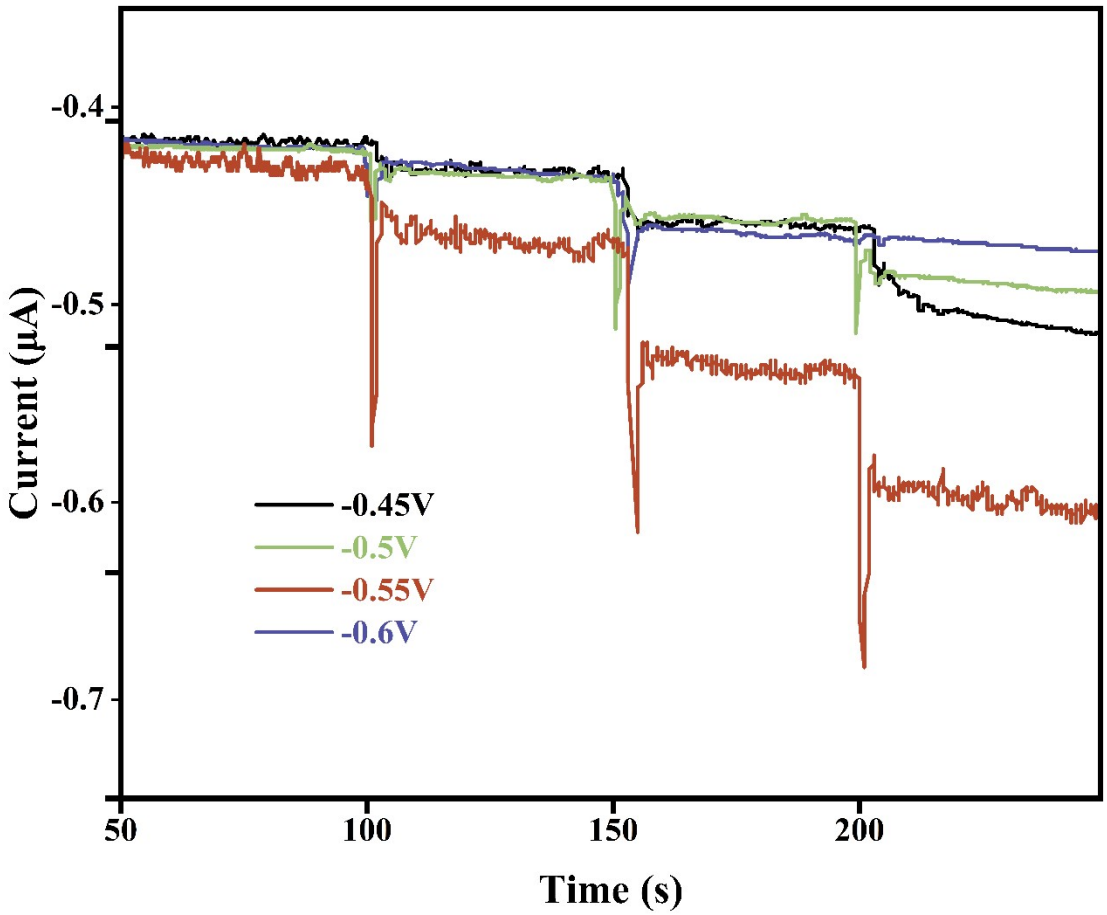

Fig. S16. Applied potential optimization for Pt-W-GO@ME I-t response toward H_2O_2.

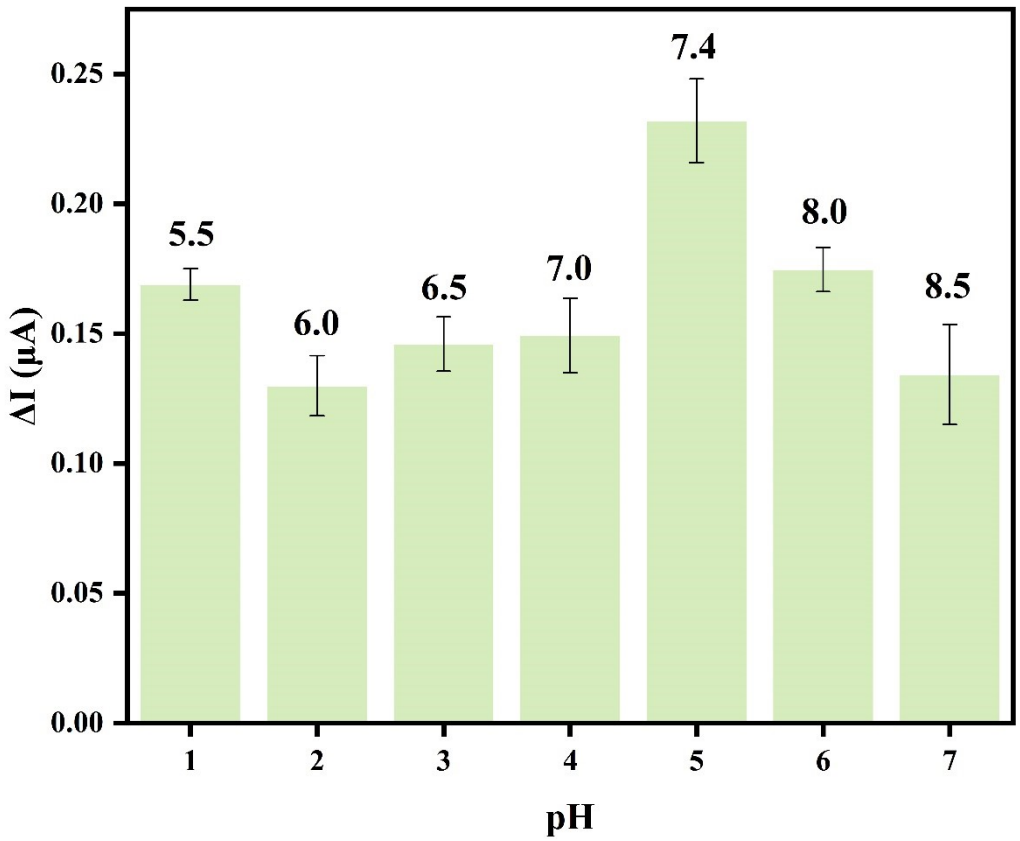

Fig. S17. Current change value of CV at different pH.

As shown in Fig. S17, 10 uL 0.088 M H_2O_2 was added to 0.01 M PBS buffer, and the pH was optimized by cyclic voltammetry. When the pH value of the phosphate buffer solution is equal to 7.4, the current response value changes the most, so it is chosen as the PBS used in the experiment.

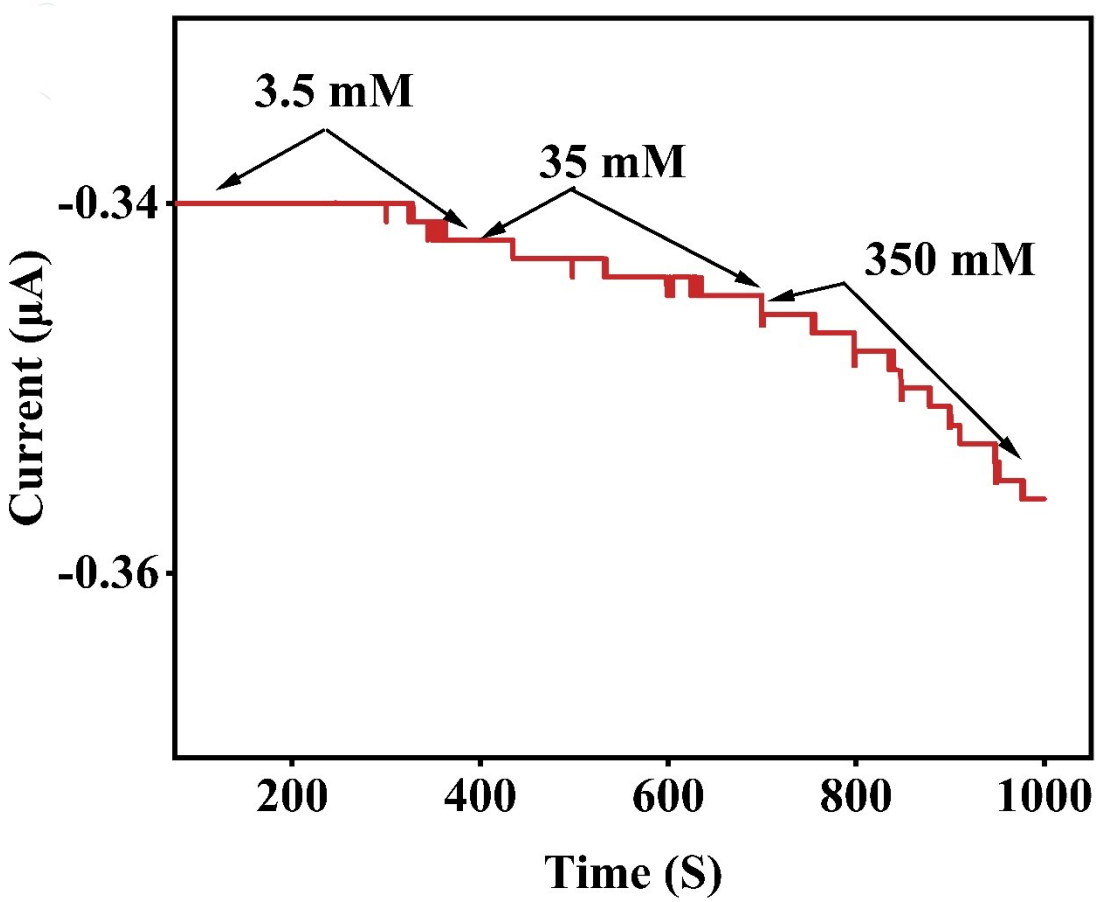

Fig. S18. The I-t curves of Pt-W-GO@ME for detection of H_2O_2.

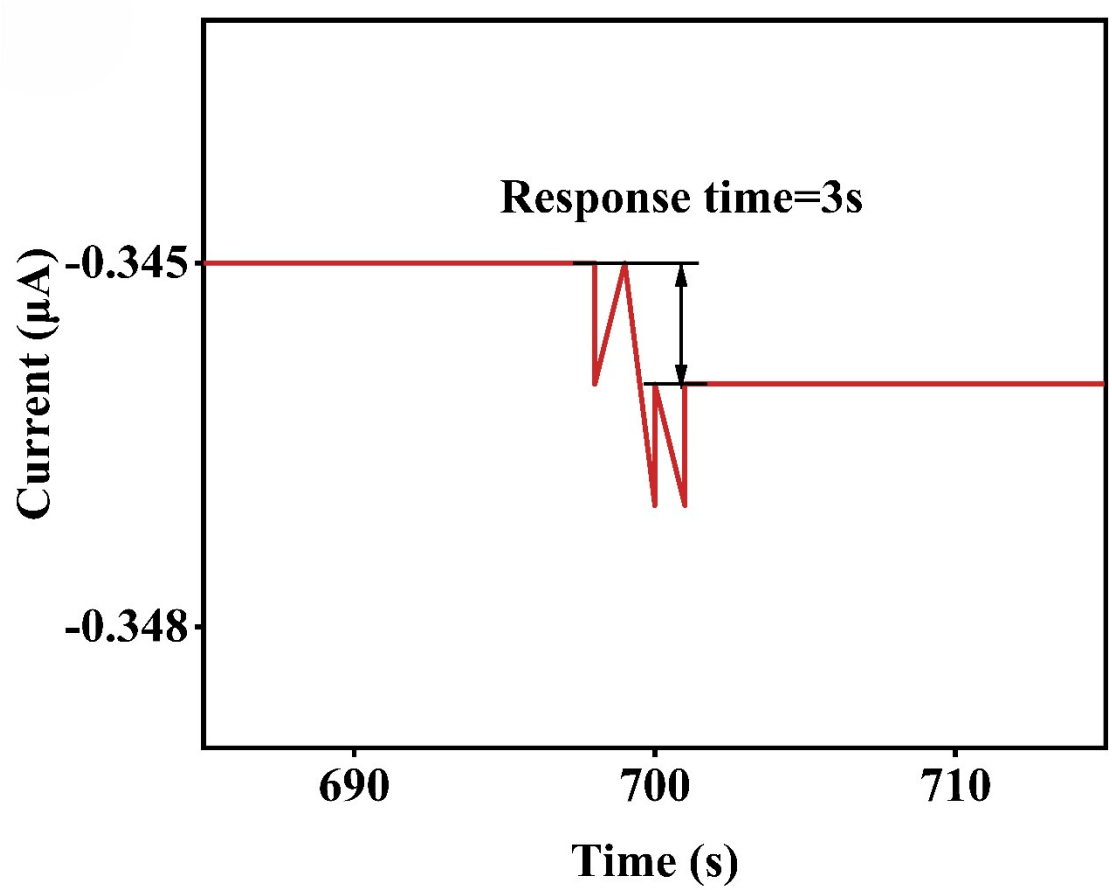

Fig. S19. Response time of the Pt-W-GO@ME toward H_2O_2.

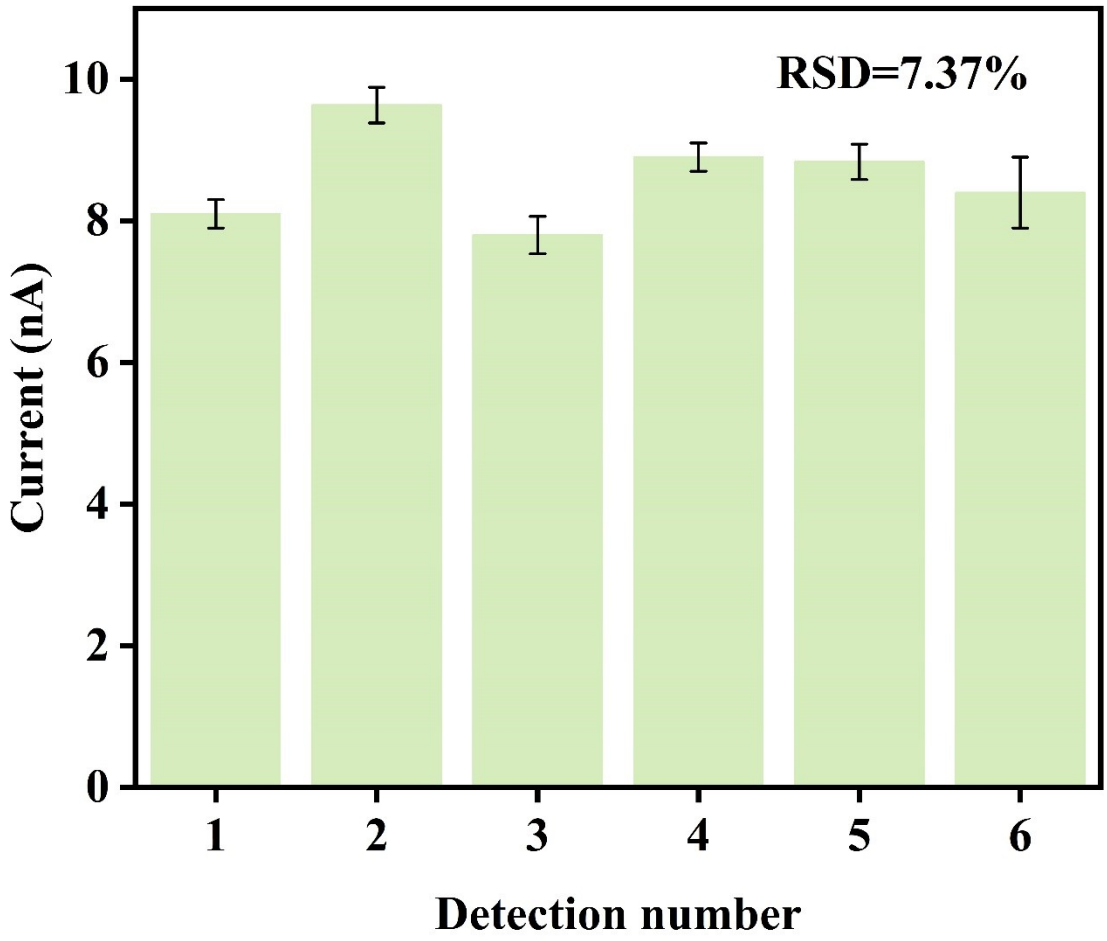

Fig. S20. Stability of Pt-W-GO@ME.

The amperometric I-t curve was recorded by adding 10 uL 0.088 M H_2O_2 into 0.01 M PBS buffer (Fig. S20). The Pt-W-GO@ME stored at room temperature was tested on day 1, day 3, day 7, day 16, day 23, and day 30 respectively, and the stability data were obtained. The stability of the microelectrode sensor is good, and it still has good performance after one month.

Table S1. Comparison of the performance of the different materials and this work.

Materials	**Linear range (μM)**	**LOD (μM)**	**Sensitivity (μA mM^{-1} cm^{-2})**	**Ref.**
Pt-W-GO@ME	3.5~3184.65	1.17	13921.75, 3393.99	This work
Au/Pt/$Ti_3C_2Cl_2$	50~10000	10.24	—	1
Pt_{21}/RGO/Nafion/GCE	1~1477	0.50	341.14	2
Cytochrome c	20~240	14.6	—	3
Hb/CMC-TiO_2 nanotubes	4~64	4.637	—	4
FTO/Fe_2O_3NR/$FePO_4$	6.6 ~ 2500	1.3	—	5
MoS_2-Au-Ag	50~20000	—	405.24	6
PdPt NCs@SGN	1~300	0.3	—	7
Ag@TiO_2	8.3~43.3	0.83	65.23	8

The process of cell detection by microelectrode under inverted microscope.mp4

Video. S1. The process of microelectrode detection at cellular scale under microscope.

References

1. X. Xi, J. Wang, Y. Wang, H. Xiong, M. Chen, Z. Wu, X. Zhang, S. Wang and W. J. C. Wen, 2022, **197**, 476-484.
2. J. Liu, X. Bo, Z. Zhao, L. J. B. Guo and Bioelectronics, 2015, **74**, 71-77.
3. L. J. B. Zhang and Bioelectronics, 2008, **23**, 1610-1615.
4. W. Zheng, Y. Zheng, K. Jin and N. J. T. Wang, 2008, **74**, 1414-1419.
5. C.-Y. Lin, C.-T. J. S. Chang and A. B. Chemical, 2015, **220**, 695-704.
6. J. Hu, C. Zhang, X. Li and X. J. S. Du, 2020, **20**, 6817.
7. Y. Fu, D. Huang, C. Li, L. Zou and B. J. A. c. a. Ye, 2018, **1014**, 10-18.
8. M. M. Khan, S. A. Ansari, J. Lee, M. H. J. M. S. Cho and E. C, 2013, **33**, 4692-4699.